

Live-fly experimentation for pigeon-inspired obstacle avoidance of quadrotor unmanned aerial vehicles

Mengzhen HUO, Haibin DUAN*, Qing YANG, Daifeng ZHANG & Huaxin QIU

Science and Technology on Aircraft Control Laboratory, School of Automation Science and Electrical Engineering, Beihang University (BUAA), Beijing 100191, China

Received 26 June 2018/Accepted 10 July 2018/Published online 3 April 2019

Abstract In this paper, we applied a pigeon-inspired obstacle-avoidance model to the flight of quadrotor UAVs through environments with obstacles. Pigeons bias their flight direction by considering the largest gap and minimum required steering. Owing to the similarities between pigeon flocks and UAV swarms in terms of mission requirements, the pigeon-inspired obstacle-avoidance model is used to control a UAV swarm so that it can fly through a complex environment with multiple obstacles. The simulation and flight results illustrate the viability and superiority of pigeon-inspired obstacle avoidance for quadrotor UAVs.

Keywords UAV swarm, pigeon flock, pigeon-inspired model, obstacle-avoidance, live-fly experimentation

Citation Huo M Z, Duan H B, Yang Q, et al. Live-fly experimentation for pigeon-inspired obstacle avoidance of quadrotor unmanned aerial vehicles. *Sci China Inf Sci*, 2019, 62(5): 052201, <https://doi.org/10.1007/s11432-018-9576-x>

1 Introduction

Recently, the unmanned aerial vehicles (UAVs) have received greater attention owing to its increasing utilization in military and civilian fields, especially in local conflicts. Obstacle avoidance is crucial for UAVs while performing tasks at high speed. To date, studies on UAV obstacle avoidance have been widely conducted with much research focusing on modeling and solution methods. The approaches can be divided into three categories: stereo vision based on sensors [1–3], stereo vision based on onboard cameras [4], and algorithms for UAV path planning with obstacle avoidance [5, 6]. Considering the limitations of UAV take-off weight and real-time performance during battles, the above methods cannot always satisfy the requirements.

Similar to a UAV swarm, many flying animals have evolved impressive abilities to avoid collisions with obstacles [7]. Birds fly around buildings, street lamps and vehicles with proficiency and depend on vision to navigate through the environments with obstacles. For example, echolocation is used by big brown bats to avoid obstacles while tracking flying insects at night, and goshawks chase prey through dense woodlands at high speed. Flight models based on birds have been developed widely by researchers for application to UAV swarms [8–10].

Among birds, pigeons have successfully colonized cities, which are highly three-dimensional environments [11]. Pigeons have a wide panoramic field of view for predator detection. Hence, Lin et al. [12] examined short-range guidance of pigeons flying through randomized sets of vertical obstacles to establish a flight model for obstacle avoidance. They concluded that pigeons must first identify relevant obstacles

* Corresponding author (email: hbdan@buaa.edu.cn)

and then select a suitable gap aim. The strategy of gap selection is generally decomposed into two concurrent and possibly competing objectives [13]: maximizing clearance between obstacles and minimizing required steering. That is, pigeons do not simply steer to the nearest opening along their flight direction or towards their destination. They bias their flight direction towards larger visual gaps while making fast steering decisions. This behavioural model converts obstacle avoidance behavior into a target-aiming behavior, which is easier to implement in UAVs. Owing to the similarity between pigeons and UAVs in terms of mission requirements, the pigeon obstacle-avoidance model is applied to control UAVs in this study, enabling them to fly through a complex environment with multiple obstacles [14]. However, the contributions of this paper also include the technologies supporting UAV testbed in frastructure.

The rest of the paper is organized as follows. Section 2 models the behavior of pigeons to safely fly to their destination in an environment with obstacles and maps the model to a UAV swarm. The system architecture of UAVs is presented in Section 3, including a description of the hardware, software and network that enable field tests of this magnitude. Simulation and flight results and a discussion of the data are shown in Section 4. Our concluding remarks are summarized in Section 5, along with suggestions for future research.

2 Obstacle avoidance model

2.1 Pigeon obstacle-avoidance model

In this paper, we consider three obstacle avoidance procedures: (i) identifying the obstacles, (ii) selecting suitable gap, and (iii) implementing steering. As shown in Figure 1, pigeons first identify obstacles through visual perception, and pigeons have limited visual perception that fall within $\pm 45^\circ$ of the flight direction. Therefore, the current obstacles within the field of view are three trees labeled numbered 1 through 3. Considering visual gaps and steering, pigeons subsequently aim their flight direction towards a larger gap with minimized required steering. It is obvious that $\theta_1 > \theta_2$, and steering must be minimized by a steering controller. Finally, pigeons aim their flight direction and fly through the obstacles.

The steering controller used here is designed as follows. According to flight guidance conventions [15], a pigeon's flight direction angular velocity $\dot{\theta}_{\text{pigeon}}$ is set as the control variable. We construct a simple PID controller with a visuomotor delay τ and three constant steering gains: proportional gain for steering K_P , integral gain for steering K_I , and derivative gain for steering K_D . This steering controller is modeled as follows:

$$\dot{\theta}_{\text{pigeon}}(t) = K_P \cdot \theta(t - \tau) + K_I \cdot \int \theta(t - \tau) dt + K_D \cdot \dot{\theta}(t - \tau), \quad (1)$$

where t is time and θ_{pigeon} is the flight direction. θ is the angular deviation from the steering aim θ_{aim} given by

$$\theta = \theta_{\text{pigeon}} - \theta_{\text{aim}}. \quad (2)$$

The flight direction at the next time is updated by

$$\theta(t + 1) = \theta_{\text{pigeon}} + \dot{\theta}_{\text{pigeon}}(t). \quad (3)$$

The controller parameters are continuously adjusted to obtain a smooth and stable obstacle-avoidance path. For comparison, a more conventional obstacle repulsion model similar to that in [16] was fit into our steering controller. During flight, obstacles have tendency to change as they are approached. Then, the appropriate steering is calculated using

$$\alpha_i = (\theta_{\text{pigeon}} - \theta_i) \cdot \frac{\theta_{\text{th}}}{\theta_{\text{pigeon}} - \theta_i} \cdot \frac{R_{\text{th}}}{R_i}, \quad (4)$$

where α_i is the desired steering aim relative to the obstacle to avoid, θ_i is the angular location of the obstacle, R_i is the distance from the obstacle, θ_{th} is the angular threshold, R_{th} is the detection threshold. While the obstacle is located at the edge of the detection threshold and with minimum detection distance,

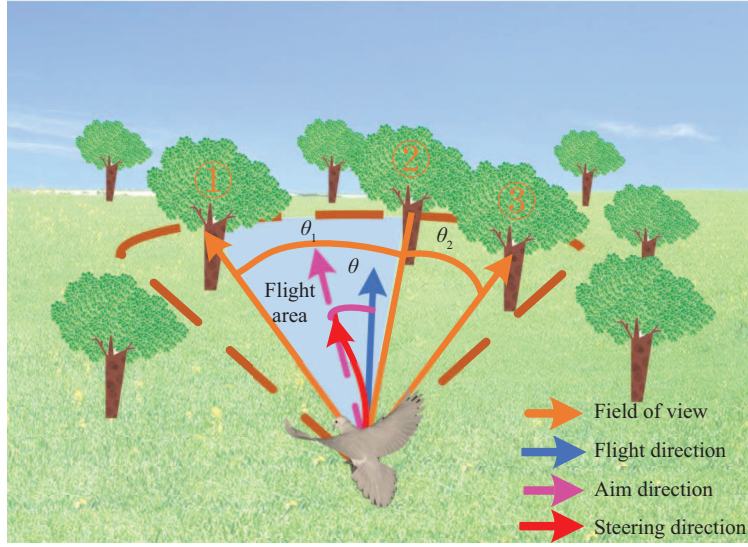


Figure 1 (Color online) Model framework of obstacle avoidance by pigeons.

α_i is equal to the difference between θ_{pigeon} and θ_i , and the steering aim becomes the pigeon's flight direction. As the obstacle distance and angle decrease, α_i increases rapidly and drives the steering away from the obstacle. When there exist multiple obstacles within the detection distance, the steering aim is

$$\theta_{\text{aim}} = \sum (\theta_i + \alpha_i). \quad (5)$$

Gaussian noise can be added to a simulation to represent the uncertainty of sensors.

2.2 UAV swarm obstacle avoidance model

Inspired by the pigeon obstacle avoidance model, we designed the obstacle avoidance algorithm for a UAV swarm. The primary steps of the algorithm are as follows:

Step 1. Get the positions of all obstacles;

Step 2. Get the self-status-message and subscribe status messages of other UAVs;

Step 3. Calculate the distances and direction angles for all obstacles, and then select the obstacles within the angular threshold θ_{th} and detection threshold R_{th} ;

Step 4. Based on the obstacle avoidance rule, (i) select the dangerous obstacle O_1 that is at the minimum distance from the UAV; (ii) calculate the gap angles between dangerous obstacles and other obstacles, and select the obstacle O_2 with the largest differential angle; (iii) set the median value of the angle between obstacle O_1 and O_2 as the steering direction;

Step 5. Avoid inertial collision: (i) calculate the distances between other UAVs, and then select dangerous UAVs within the angular threshold and safe distance; (ii) update the steering direction using the following equation:

$$\theta_{\text{aim}} = \text{atan2}(\text{hdg_y}, \text{hdg_x}), \quad (6)$$

$$\text{hdg_x} = (\cos(\theta_{\text{pigeon}}) + \cos(\theta_1) + \cdots + \cos(\theta_m))/m, \quad (7)$$

$$\text{hdg_y} = (\sin(\theta_{\text{pigeon}}) + \sin(\theta_1) + \cdots + \sin(\theta_m))/m, \quad (8)$$

where m is the number of dangerous UAVs, $\theta_1, \dots, \theta_m$ are angles between the vectors from the current UAV and other dangerous UAVs;

Step 6. Update the flight direction using Eqs. (1) and (2).

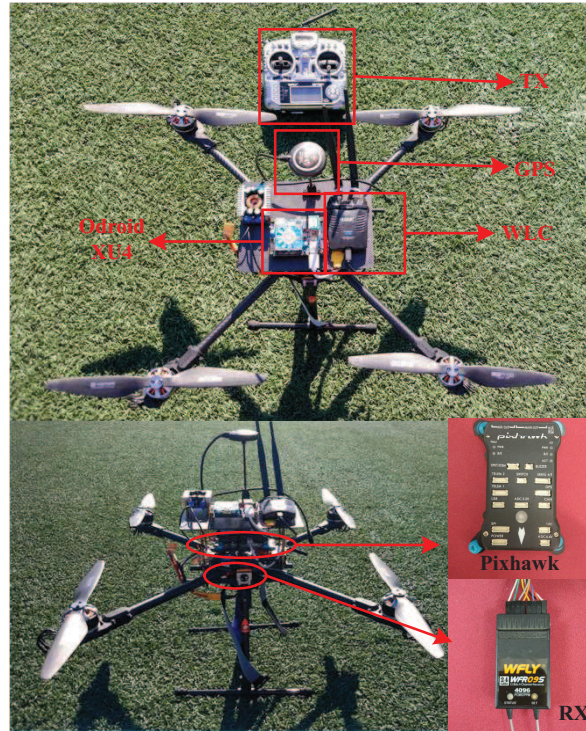


Figure 2 (Color online) UAV system components.

Table 1 List of core flight system components

Component	Version
Airframe	ProHawk 650
Avionics	Pixhawk autopilot
Autonomy CPU	Hardkernel Odroid XU4
Payload link	Ethernet, USB, WiFi, radio, adapter (2 GHz)
Power	Tiger 5200 mAh/ 11.1 V/ 25 C/ 4 S
Propulsion	T-Motor U-Power U3 700 KV
ESC	T-Motor 40 A
GPS/Compass	3DR UBLOX NEO-M8N
RC TX/RX	WFT-0SII and WFR09S

3 System architecture

3.1 Flight system

Figure 2 shows the ProHawk 650 quadrotor UAV. The airframe selection was driven by several criteria of varying significance, including: mission capability, size, weight, flight speed, configuration, endurance, and cost, among others. The primary components are listed in Table 1.

3.2 Software systems

As Figure 3 shows, the Odroid XU4 payload computer links to the Pixhawk through USB ports, sends task instructions via the Mavlink protocol, and receives flight status simultaneously. The ground station is a software, named Mission Planner, which communicates with UAVs through a data transfer unit. Wireless lan card generates wifi signal and establishes a communication network. The transmitter is read via the S-BUS protocol.

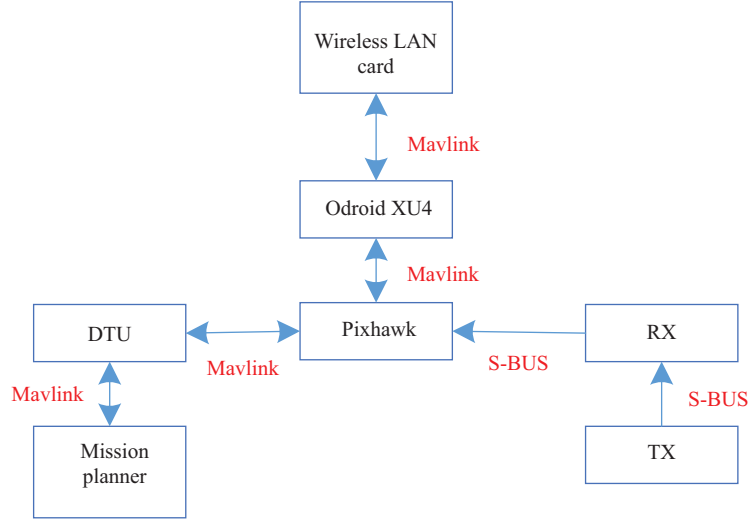


Figure 3 (Color online) The software platform.

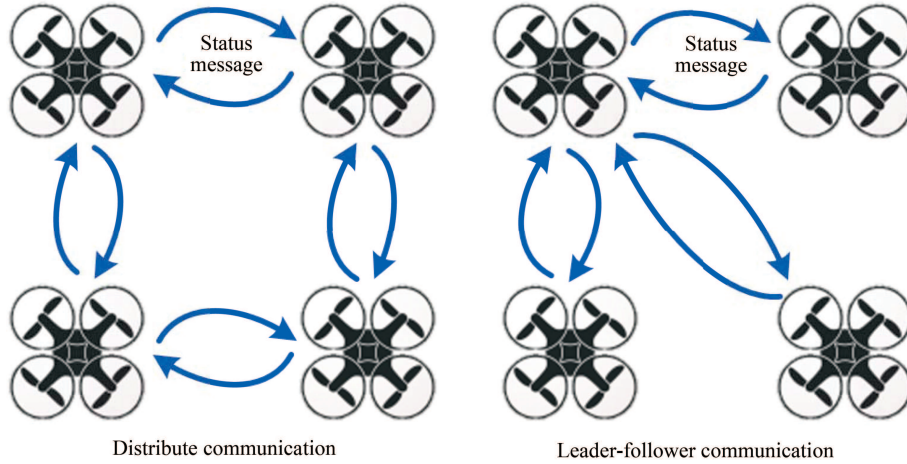


Figure 4 (Color online) Communication mode.

3.3 Communication system

In our experimentation, a distributed communication network is used for communication in the UAV swarm. A robot operating system (ROS) is an open-source framework originally created for building robotic software [17]. It consists of libraries, tools, and conventions which greatly simplify the task of building a complex robotic system. Due to the open source nature of the framework, ROS has an increasing number of different tools which make interfacing with different sensors and devices much easier [18]. In our experiments, the publish-subscribe model in ROS was used to support communication between UAVs. All UAVs adopt the broadcast mode to publish the flight status (latitude, longitude, altitude, heading, velocity, and so on) and subscribe the message from other UAV.

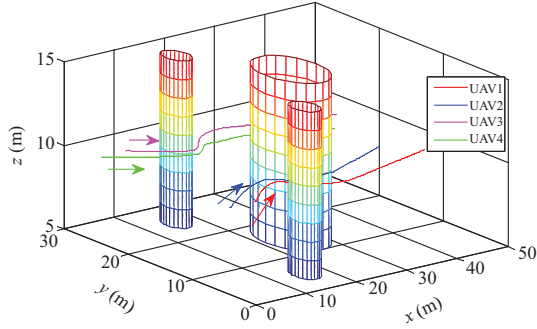
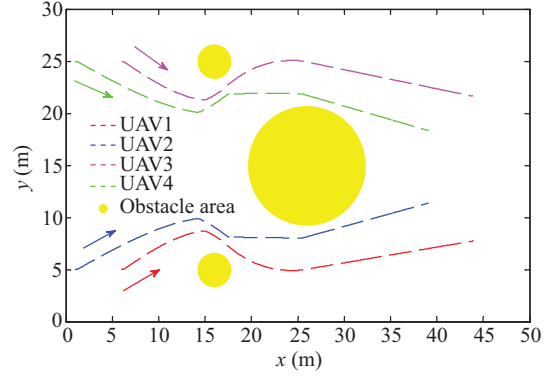
Compared to the leader-follower communication network, as shown in Figure 4, a distributed communication network can obtain more comprehensive and accurate flight information in the line of duty, which improves network stability.

Table 2 Initial states

Variable	Description	Values
P_{UAV}	Position of the UAV swarm	[1, 5, 10], [1, 25, 10], [6, 5, 10], [6, 25, 10]
P_{obstacle}	Position of the centers of obstacle areas	[16, 5, 10], [16, 25, 10], [26, 15, 10]
ϕ_{UAV}	Heading angle of the UAV swarm	$[0^0, 0^0, 0^0, 0^0]$

Table 3 Parameter setting

Parameter	Description	Value
θ_{th}	Angular threshold	$\pm 45^\circ$
R_{th}	Detection threshold	20 m
N_{UAV}	Number of UAVs	4
N_{obstacle}	Number of obstacles	3
V_{UAV}	UAV flight speed	0.1 m/s
T	Simulation time	500 s

**Figure 5** (Color online) Three-dimension simulation results.**Figure 6** (Color online) Plan view of the simulation results.

4 Experimental results

4.1 Simulation test

In the simulation, the UAV swarm is expected to avoid three target areas based on the obstacle-avoidance algorithm with multiple goals, consisting of avoiding targets, maintaining formation, and maintaining airspeed. The initial states of the UAV swarm are shown in Table 2. The control parameters are listed in Table 3. The kinestates of the UAV swarm are subsequently updated using (6). The simulated flight paths of the UAV swarm are shown in Figures 5 and 6.

As one can see in Figures 5 and 6, the obstacle areas are represented by three cylinders and three circles, respectively. It is clear that the UAV swarm could always stay a safe distance from the obstacles and maintain a stable formation simultaneously. Figure 7 shows how the heading angle changes. The data reflects that the maximum turning rate occurs after 420 s. The maximum turning rate is approximately equal to 0.0565 rad/s (3.24 degree/s), which is less than the maximum allowed turning rate value. As the airspeed vector varies with steering direction, it is easy to maintain airspeed at a constant value during the simulation.

4.2 Live-fly experimentation

During flight experiments, the obstacle avoidance algorithm is coded into the Odroid XU4 payload computer in each UAV. Pixhawk can receive commands from the Odroid, thus controlling the flight of the UAV, and the UAV status is fed back to the Odroid. The UAV swarm formation during flight experiment is shown in Figure 8. During flight experiments, the mission of UAV1 and UAV2 is to detect and avoid

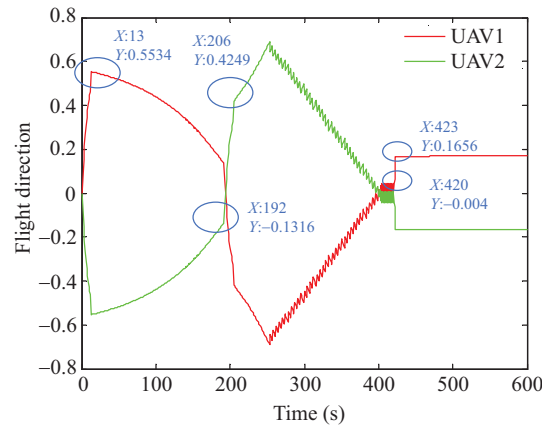


Figure 7 (Color online) Flight direction of the UAVs.



Figure 8 (Color online) Flight scene of the UAV swarm.

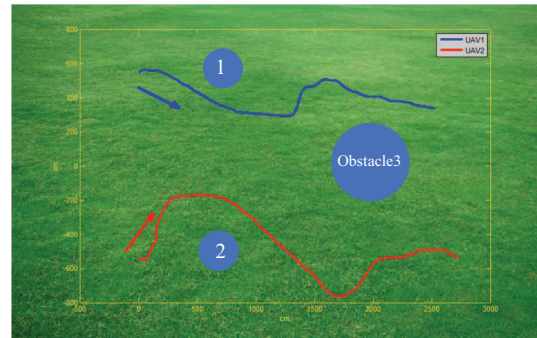


Figure 9 (Color online) Flight path of the UAV swarm.

obstacles, while the tasks of UAV3 and UAV4 are primarily tracking the paths of UAV1 and UAV2, as well as avoiding collisions with other UAVs. Information on obstacles is transferred to the UAVs by the ground station.

Figure 9 is shown using the flight data for two quadrotor UAVs, which primarily perform the task of avoiding obstacles. The flight data is obtained from the Mission Planner connected to the Pixhawk. Because the flight data contains the latitude and longitude of the UAVs, the points in Figure 9 are obtained by calculating the relative distance between the initial point and other flight points in order to make the flight path more visible. As one can see in Figure 9, the experimental flight trajectory is similar to that from a simulation test. At beginning, two UAVs could detect obstacle1 and obstacle2 in front of them and change course to avoid both obstacles. Then, the UAVs fly forward until obstacle3 is detected. The UAVs update their optimal steering direction using the obstacle avoidance algorithm. When there is no obstacle within the angular threshold and detection threshold, the UAVs would fly back on their original course. The flight paths in Figure 9 show that the UAVs fly safely through the obstacles without collisions, and our proposed pigeon-inspired obstacle avoidance model is shown to be viable.

The flight path in Figure 9 is not as smooth as that in Figure 6, possibly due to the following reasons:

(1) The simulation test does not consider weather disturbances during flight. During flight experiments, the UAV swarm might be influenced by the wind or other disturbances.

(2) During flight experiments, GPS location is not accurate, which guides the UAVs to a position deviated from the correct position.

(3) Communication between the UAVs has a time delay, which could not be eliminated by the steering controller.

5 Conclusion

The use of UAV swarms enhances the ability to control battle-field situations, but it also requires significant investments in obstacle avoidance technologies owing to the large scale of UAV deployments. As there is some similarities between pigeon flocks and UAV swarms in terms of their mission requirements, the pigeon-inspired obstacle avoidance model was used to guide UAV swarms. The simulation results illustrate the successful application to a UAV swarm in an environment with obstacles, and the measured data also reflects the viability of the obstacle avoidance model. The live-fly results show that the UAV swarm could fly through multiple obstacle areas and avoid collisions with other UAVs in a real flight environment. Although we have shown that our proposed model is viable, it must be further optimized. We will also develop further theoretical research on obstacle avoidance and its application to UAV swarm control in order to promote the emergent intelligence of unmanned systems.

Acknowledgements This work was supported by National Natural Science Foundation of China (Grant Nos. 61425008, 61333004, 91648205).

References

- 1 Chen Z Y, Luo X Y, Dai B C. Design of obstacle avoidance system for micro-UAV based on binocular vision. In: Proceedings of International Conference on Industrial Informatics – Computing Technology, Intelligent Technology, Industrial Information Integration, Wuhan, 2017. 67–70
- 2 Meng G L, Pan H B. The application of ultrasonic sensor in the obstacle avoidance of quad-rotor UAV. In: Proceedings of Guidance, Navigation and Control Conference, Nanjing, 2016. 976–981
- 3 Yang Y, Wang T T, Chen L, et al. Stereo vision based obstacle avoidance strategy for quadcopter UAV. In: Proceedings of Chinese Control and Decision Conference, Shenyang, 2018
- 4 Peng X Z, Lin H Y, Dai J M. Path planning and obstacle avoidance for vision guided quadrotor UAV navigation. In: Proceedings of IEEE International Conference on Control and Automation, Kathmandu, 2016. 984–989
- 5 Zhao Y J, Zheng Z, Zhang X Y, et al. Q learning algorithm based UAV path learning and obstacle avoidance approach. In: Proceedings of Chinese Control Conference, Dalian, 2017. 3397–3402
- 6 Cekmez U, Ozsiginan M, Sahingoz O K. Multi colony ant optimization for UAV path planning with obstacle avoidance. In: Proceedings of International Conference on Unmanned Aircraft Systems, Arlington, 2016. 47–52
- 7 Norberg U M. Vertebrate flight: mechanics, physiology, morphology, ecology and evolution. *Comp Biochem Phys Part A-Phy*, 1990, 96: 529
- 8 Qiu H X, Wei C, Dou R, et al. Fully autonomous flying: from collective motion in bird flocks to unmanned aerial vehicle autonomous swarms. *Sci China Inf Sci*, 2015, 58: 128201
- 9 Luo Q N, Duan H B. An improved artificial physics approach to multiple UAVs/UGVs heterogeneous coordination. *Sci China Technol Sci*, 2013, 56: 2473–2479
- 10 Zhang T J. Unmanned aerial vehicle formation inspired by bird flocking and foraging behavior. *Int J Autom Comput*, 2018, 15: 402–416
- 11 Baptista L, Trail P, Horblit H. Family columbidae. In: *Handbook of the Birds of the World*. Barcelona: Lynx Edicions, 1997
- 12 Lin H T, Ros I G, Biewener A A. Through the eyes of a bird: modelling visually guided obstacle flight. *J R Soc Interface*, 2014, 11: 20140239
- 13 Moussaid M, Helbing D, Theraulaz G. How simple rules determine pedestrian behavior and crowd disasters. *Proc Natl Acad Sci USA*, 2011, 108: 6884–6888
- 14 Qiu H X, Duan H B. Pigeon interaction mode switch-based UAV distributed flocking control under obstacle environments. *ISA Trans*, 2017, 71: 93–102
- 15 Land M F, Collett T S. Chasing behaviour of houseflies (*fannia canicularis*). *J Comp Physiol*, 1974, 89: 331–357
- 16 Warren W H, Fajen B R. Behavioral dynamics of visually guided locomotion. In: *Coordination: Neural, Behavioral and Social Dynamics*. Berlin: Springer, 2008. 45–75
- 17 Foundation O S R. Robot operating system. <http://www.ros.org/about-ros/>
- 18 Rokonzaman M, Amin M A A, Ahmed M H K M U, et al. Automatic vehicle identification system using machine learning and robot operating system (ROS). In: Proceedings of the 4th International Conference on Advances in Electrical Engineering (ICAEE 2017), Dhaka, 2017. 253–258